WASHINGTON STATE DEPARTMENT OF
Natural Resources
Doug Sutherland - Commissioner of Public Lands
Division of Geology and Earth Resources
Ron Teissere - State Geologist

Geologic Map of the Elwha and Angeles Point 7.5-minute Quadrangles, Clallam County, Washington

by Michael Polenz, Karl W. Wegmann, and Henry W. Schasse

June 2004

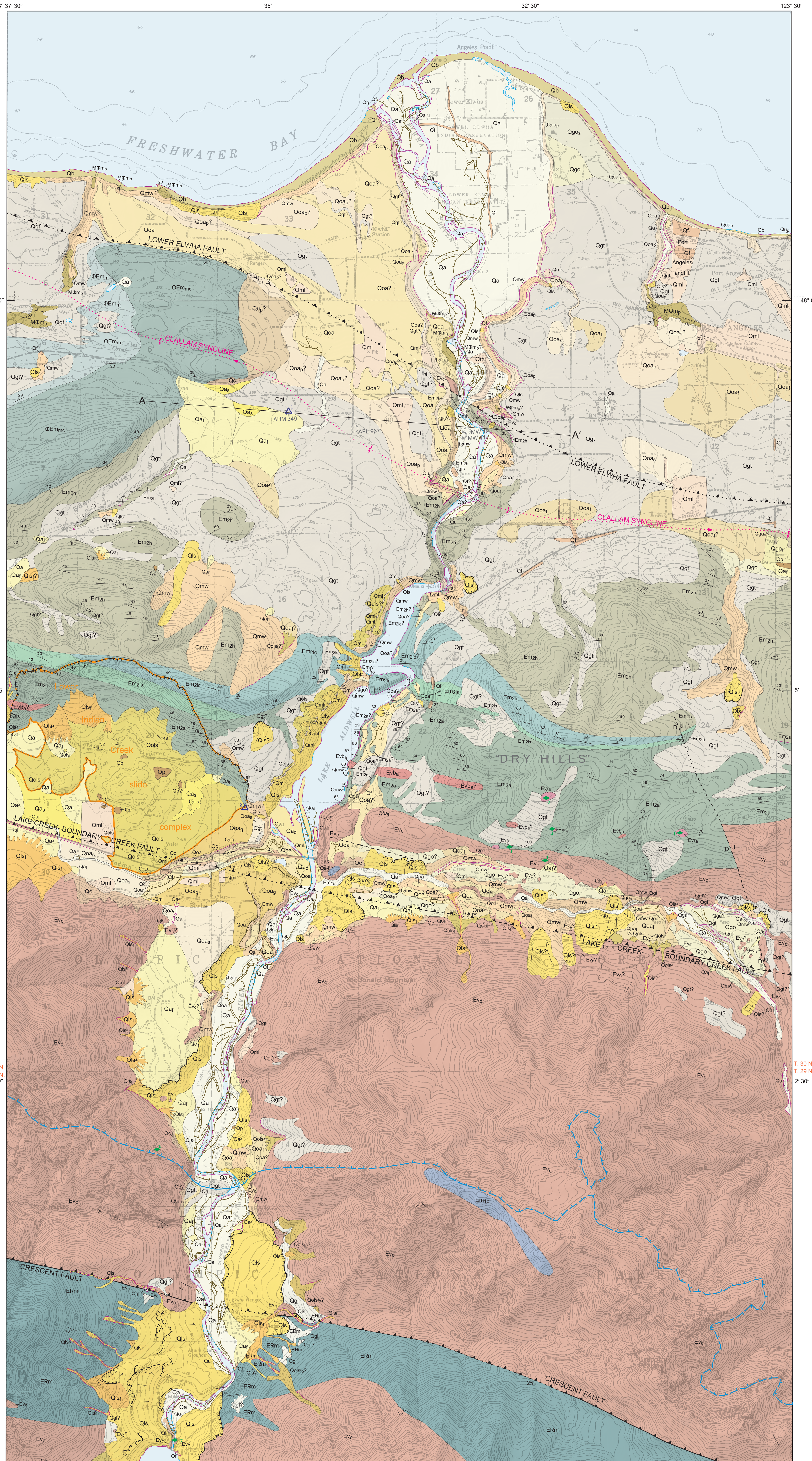

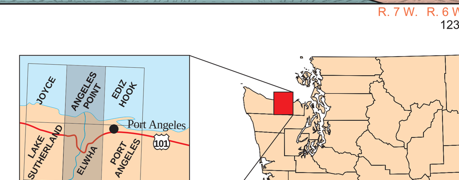

METHODS

This project was mapped concurrently with the Port Angeles and Ediz Hook quadrangles (Schasse and others, 2004), which assisted us in our interpretation of geologic structure and Quaternary units. We used a digital elevation model (DEM) based on lidar data from the Puget Sound Lidar Consortium (http://rocky2.ess.washington.edu/data/raster/lidar/index.htm) to identify landforms and map geologic contacts with a level of confidence not previously attainable in densely vegetated or inaccessible areas. We believe that contacts are within about 200 ft of their shown location. To make our mapping consistent with conditions implied by the underlying basemap, we adjusted some contacts where the basemap is inaccurate, such as along the Elwha River. Consequently, some contacts are shifted up to 550 ft from their true location. These contacts are identified by purple contact lines. We used selected water well logs supplied by the Washington Department of Ecology to interpret structure and subsurface geology.

We used the geologic time scale of the Correlation of Stratigraphic Units of North America Project of the American Association of Petroleum Geologists (Salvador, 1985), with boundary-age modifications of Montanari and others (1985). We use 'ka' to mean thousands of calendar years before A.D. 1950. We identify radiocarbon years by the term '^{14}C'. We conform data provided by other workers to the same terminology, unless we are unsure of their meaning, in which case we report their terminology in quotation marks.

Some volcanic rocks are identified using whole-rock geochemistry and total-alkali silica diagrams (Zanettin, 1984). Sandstones are named using the classification scheme of Dickinson (1970). Most of our bedrock linework and interpretations differ little from those of Brown and others (1960) and the regional summaries of Tabor (1975) and Tabor and Cady (1978a,b). We agree with Schasse (2003) in inferring faulting not shown by Tabor and Cady. Our other revisions pertain mostly to the Quaternary sediments. We sought to map Quaternary units where they mask the underlying units and appear to be thick enough to be of geotechnical significance, generally 5 ft or thicker.

GEOLOGIC SETTING AND DEVELOPMENT

Tertiary sedimentary rocks of the upper Eocene to lower Miocene Twin River Group and the middle Eocene Aldwell and Lyre Formations overlie the early to middle Eocene Crescent Formation and Blue Mountain unit in the map area. We agree with Snavely and others (1978) in referring to the upper, middle and lower members of the Twin River Group (Twin River Formation of Brown and Gower, 1958, and Brown and others, 1960) as the Pysht, Makah, and Hoko River Formations. The Tertiary units are folded and thrust-faulted together by post-early Miocene tectonism. For a north–south bedrock cross section, see Schasse and others (2004).

Late Quaternary sediments thinly and discontinuously drape the foothills below 1500 ft elevation and locally thicken to several hundred feet in the coastal plain (Wash. Dept. of Ecology, 1978; K. L. Othberg and R. L. Logan, [illegible] better sorted, and more mature than Olympic sand.

CONCEPTUAL MODEL OF LATE QUATERNARY LANDSCAPE DEVELOPMENT

The modern landscape was formed by the interaction of the Juan de Fuca lobe (**JFL**) of the late Wisconsinan glaciation and the Elwha River. JFL till (unit Qgt) discontinuously conceals JFL advance outwash (unit Qga), older sediments, and bedrock. The Pleistocene Elwha River delta fan consists almost entirely of a thick sheet of compact Olympic gravel (unit Qoa_p) with less than 1 percent northern sediment. Unit Qoa_p is discontinuously covered by till that is rarely underlain by advance outwash and is locally dominated by Olympic clasts. This suggests that Olympic sediment overwhelmed the glacial input, and drift was, to some extent, diverted away from the Elwha River delta region by Elwha River sediment. The scarcity of northern sediment above unit Qoa_p, coupled with a relative abundance of northern sediment beneath unit Qoa_p, further suggests that some time prior to the late Wisconsinan glaciation, the lower Elwha followed a different course.

Continental ice advanced to roughly the 3800-ft contour along the mountain front (Long, 1975) and 2.3 mi south of the Little River in the Elwha valley, where it deposited a 100-ft-high terminal moraine. South of this moraine, Long (1975) interpreted as till what we believe to be glaciolacustrine sediments, and Long thus mapped the Elwha valley ice limit south of the Elwha quadrangle. Most workers appear to favor a JFL ice advance at about 17 ^{14}C ky B.P. and recession at about 14.5 to 14 ^{14}C ky B.P. (Fig. 1; Anderson, 1968; Heusser, 1973; Petersen and others, 1983; Waitt and Thorson, 1983). Blunt and others (1987) favor an advance some time "after 17,000 years ago". We did not find Olympic alpine drift in the map area. Sediment of Olympic provenance arguably must include alpine glacial outwash, but because we can not distinguish it from other Olympic alluvium, we have reserved the terms 'glacial', 'outwash', 'drift', etc., to deposits associated with JFL ice (except in the unit description for Qoa_p).

Because JFL ice failed to override most of the Elwha watershed, outwash in the lower Elwha valley was quickly covered by alluvium (unit Qoa). Terrace grading along the Little River valley suggests that some outwash deposition away from the Elwha valley was coeval with deposition of unit Qoa in the Elwha valley. Such coeval deposition and mixing of units Qoa and Qgo are further supported by data of Heusser (1973), who suggests that some JFL ice may not have melted until after 8 ^{14}C ky B.P. (~8.8–9 ka). Deposition of unit Qgo began with locally ice-free conditions some time between 14,460 ±200 and 12,000 ±310 ^{14}C yr B.P. (Heusser, 1973; Petersen and others, 1983). Outwash is now only sparsely exposed because latest Pleistocene and Holocene alluvium (units Qoa and Qa) largely obscures the outwash. Drainages were eliminated during glaciation, and new drainage networks were later established.

Glacial ice significantly depressed the crust in the region. When the ice melted, the global rise in sea level (see fig. 8 of Booth, 1987) initially outstripped crustal rebound in the field area (Mathews and others, 1970), raising relative sea level in the field area to >130 ft above modern mean sea level (**MSL**) (Dethier and others, 1995). That late Wisconsinan relative sea level maximum (**RSLM**) is recorded by deposition of glaciomarine drift (included with unit Qgo_s) to at least 125 ft above MSL. Possible deposits of glaciomarine drift at higher elevations may be concealed by younger sediments. The timing of glaciomarine drift deposition is constrained by data of Dethier and others (1995), who report a radiocarbon age of 12,600 ±200 ^{14}C yr B.P. from a shell in glaciomarine drift 19 mi east of the study area (their locality 11, fig. 2), and by beach uplift data from the Victoria area on Vancouver Island, which suggest maximum post-glacial relative sea level there at about "13,000 y B.P." (Mathews and others, 1970).

Low energy sediments on the coastal plain (units Qgo and Qoa) and extensive river terraces (unit Qoa), which are perched up to about 200 ft above the modern valley floor along the Elwha River, appear graded to the RSLM. The slope and elevation of these river terraces relative to the slope and elevation of glaciomarine drift above the sea cliffs suggest terrace grading to a base level significantly above MSL. Although ice- or landslide-damming of the lower Elwha valley could alternatively have temporarily elevated base level west of the "Dry Hills" along the lower Elwha River, field relations provide little support for such a local, lake-forming base level control. Thus, an elevated relative sea level in the area likely controlled deposition of the highest terraces of unit Qoa along the Elwha River and coeval terraces of unit Qgo in smaller basins, which suggests deposition of these terraces during the time of recessional late Wisconsinan glaciomarine drift deposition about 13.3 ka (Fig. 1; Mathews and others, 1970; Dethier and others, 1995).

After RSLM, crustal rebound in response to glacial unloading caused relative sea level to rapidly drop to about 200 ft below MSL (Fig. 1; Mosher and Hewitt, 2004), which triggered cutting of the steep-walled, modern valleys that are mostly limited to the unconsolidated deposits of the field area. The rate of rebound had to greatly outstrip global sea level rise and may have reached between 68 and 74 mm/yr to permit the rate of relative sea level drop estimated by Mosher and Hewitt (2004) at ≤58 mm/yr. Multiple river terraces (unit Qoa) dot the sidewalls of the modern valleys and record this period of incision, with higher terraces being older. Where streams are now bedrock controlled, they have since continued to incise. Close to shore, the larger valleys have an alluvial floor that broadens toward the shore, reflecting alluvial infilling (unit Qa) of deeper post-glacial valleys (Galster, 1989; Steve Evans, Pangeo, Inc., oral commun., 2004). Where streams did not incise into the coastal plain, unit Qa may locally grade down into unit Qoa. Both units Qa and Qoa stratigraphically succeed but may locally interfinger with unit Qgo.

Crustal rebound in the area was apparently mostly completed by 10.7 ka (Fig. 1) (Mosher and Hewitt, 2004, and references therein). Therefore, deposition of unit Qa as infill of the modern valley floors began at roughly 10.7 ka and continued until sea level approximated MSL at about 6 ka (Fig. 1; Mathews and others, 1970; Clague and others, 1982; Booth, 1987; Dragovich and others, 1994; Mosher and Hewitt, 2004). Since then, alluvial valleys near the shore have likely undergone little change. At the shore, the Holocene has been marked by sea level rise, shoreline erosion, and 3000 to 5000 ft of coastal retreat (Galster, 1989).

LARGE–SCALE LANDSLIDING AND STRUCTURAL GEOLOGY

Landslides are common in the map area. The Pysht Formation (unit $M\Phi m_p$) appears most slide-prone, followed by the Quaternary units (especially where glaciolacustrine sediments [unit Qgl] are present), then the Aldwell Formation (unit Em_{2a}). Landslides in Quaternary sediments below 1000 ft elevation are common all along the Elwha valley, but most extensive south of the ice limit, perhaps due to lack of compaction by JFL ice. The post-glacial Lower Indian Creek slide complex (**LICS**) on the north side of Indian Creek valley incorporates areas mapped as units Qls, Qols, Qls_f, Qa_s, Qa_f, Qp, Em_{2a}, Em_{2ls}, and Em_{2lc}. It spans 1500 ft of relief, has covered at least 1 mi^2 of valley floor with slide debris that has pushed Indian Creek to the southern valley margin, and is even more extensive in the subsurface. Slide body morphology suggests that the LICS may incorporate multiple major events. Evidence for recent activity is limited to rockfalls and debris flows in the headwall. Most debris flows are on the western flank, which lacks Lyre Formation conglomerate (unit Em_{2lc}) at the top.

Our interpretation of the bedrock structure is based in part on the structure mapped by Brown and others (1960) and Tabor and Cady (1978a), structural interpretations by MacLeod and others (1977) and Tabor (1983), and geologic structure in the adjoining Port Angeles quadrangle to the east (Schasse and others, 2004).

Four previously mapped faults and the Clallam syncline traverse the field area. The Clallam syncline is an east-southeast-trending, regional open fold across the northern third of the map area. It plunges gently east and north-west away from the Elwha River and has deformed all bedrock units in the area (Brown and others, 1960). Angular unconformities and pinching-out of several units in the north limb suggest that some folding pre-dates deposition of the upper Eocene Hoko River Formation (Brown and others, 1960).

[illegible]

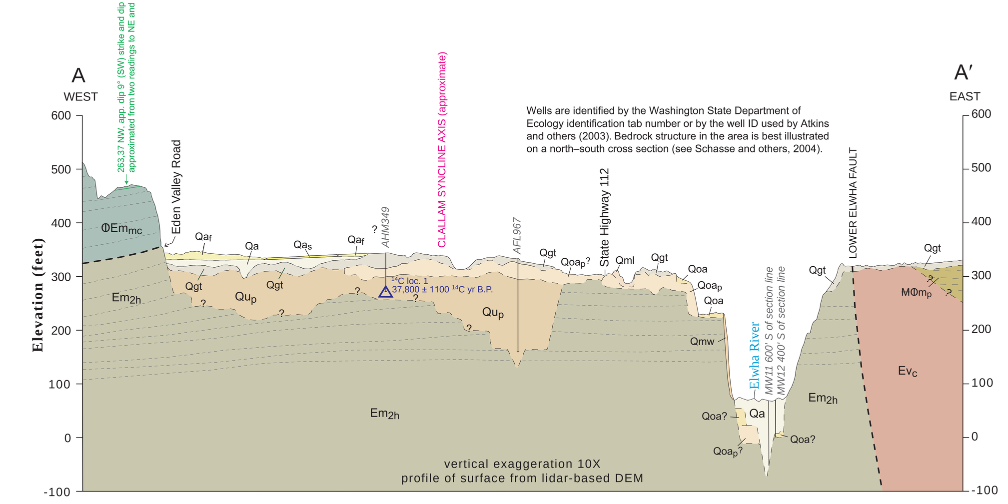

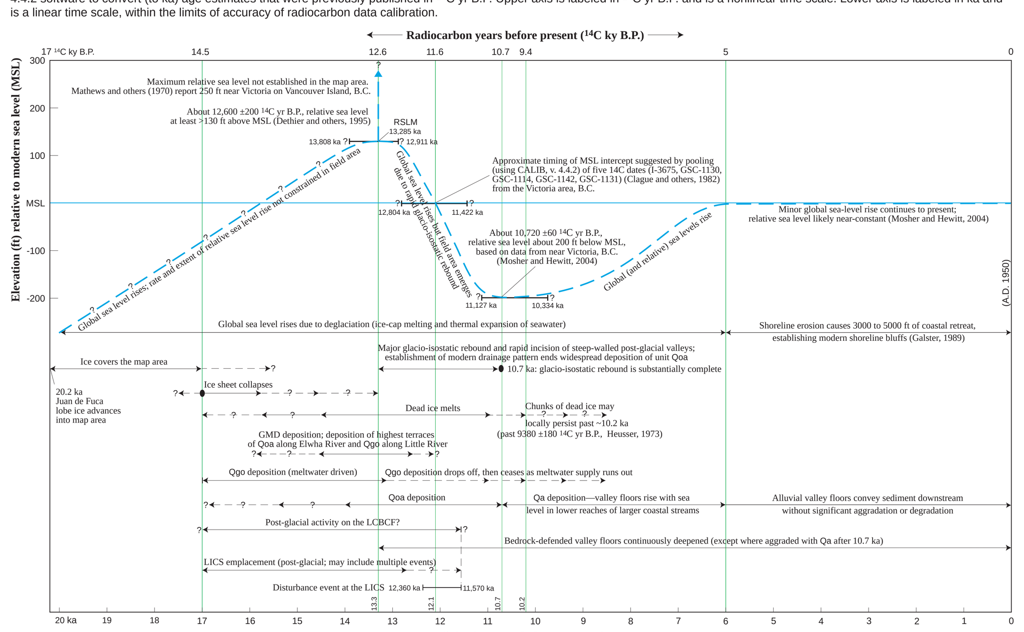

Figure 1. Relative sea level and time line of events in the field area from the late Wisconsinan glaciation to the present. [illegible]

Table 1. Geochemical analyses for the Elwha quadrangle performed by x-ray fluorescence at the Washington State University GeoAnalytical Lab. Instrumental precision is described in detail in Johnson and others (1999). Major and trace elements normalized to 100 on a volatile-free basis, with total Fe expressed as Fe; LOI%, percent loss on ignition

MAJOR ELEMENTS—NORMALIZED (weight percent)

Loc. no.	Sample no.	Geologic unit, rock type	Chemical analysis	SiO_2	TiO_2	Al_2O_3	FeO	MnO	MgO	CaO	Na_2O	K_2O	P_2O_5	Original total	LOI(%)
1	HS-49	Evr_a, rhyolite	rhyolite	74.42	0.246	12.63	3.67	0.077	1.90	0.68	5.77	0.31	0.060	99.27	– – –
2	HS-53	Evr_a, rhyolite	rhyolite	69.91	0.264	15.17	5.27	0.056	0.67	0.41	6.96	1.06	0.075	98.74	– – –
3	HS-54	Evr_a, rhyolite	dacite/rhyolite	70.70	0.298	13.82	4.57	0.090	1.68	2.24	5.57	0.65	0.048	99.62	– – –
4	HS-55	Ev_c, diabase	basalt	48.14	1.651	15.40	12.05	0.202	9.46	8.81	3.49	0.49	0.151	97.28	6.15
5	HS-56	Evr_a, rhyolite	rhyolite	77.08	0.126	12.26	2.48	0.046	0.72	0.57	4.75	1.86	0.016	99.82	1.67
6	MP-98	Ev_c, basalt	basalt	49.24	1.036	14.51	12.00	0.211	8.25	11.75	2.42	0.33	0.102	98.92	– – –
7	MP-35	Ev_c, diabase	basalt	49.29	1.124	13.99	12.88	0.271	8.53	10.74	2.93	0.03	0.088	98.15	– – –

TRACE ELEMENTS—NORMALIZED (parts per million)

Loc. no.	Sample no.	Geologic unit, rock type	Chemical analysis	Ni	Cr	Sc	V	Ba	Rb	Sr	Zr	Y	Nb	Ga	Cu	Zn	Pb	La	Ce	Th
1	HS-49	Evr_a, rhyolite	rhyolite	8	4	8	4	1088	6	195	586	94	23.6	19	8	160	5	18	41	5
2	HS-53	Evr_a, rhyolite	rhyolite	6	7	7	6	324	16	153	657	117	31.2	30	2	181	5	22	49	5
3	HS-54	Evr_a, rhyolite	dacite/rhyolite	31	54	11	37	2187	10	245	431	124	24.5	24	21	158	4	24	59	3
4	HS-55	Ev_c, diabase	basalt	91	242	44	316	73	7	235	117	33	9.0	19	136	91	2	4	24	1
5	HS-56	Evr_a, rhyolite	rhyolite	6	4	3	6	192	38	43	303	77	69.8	21	10	80	2	14	32	10
6	MP-98	Ev_c, basalt	basalt	90	264	49	369	53	5	142	64	28	2.8	16	168	91	3	7	10	0